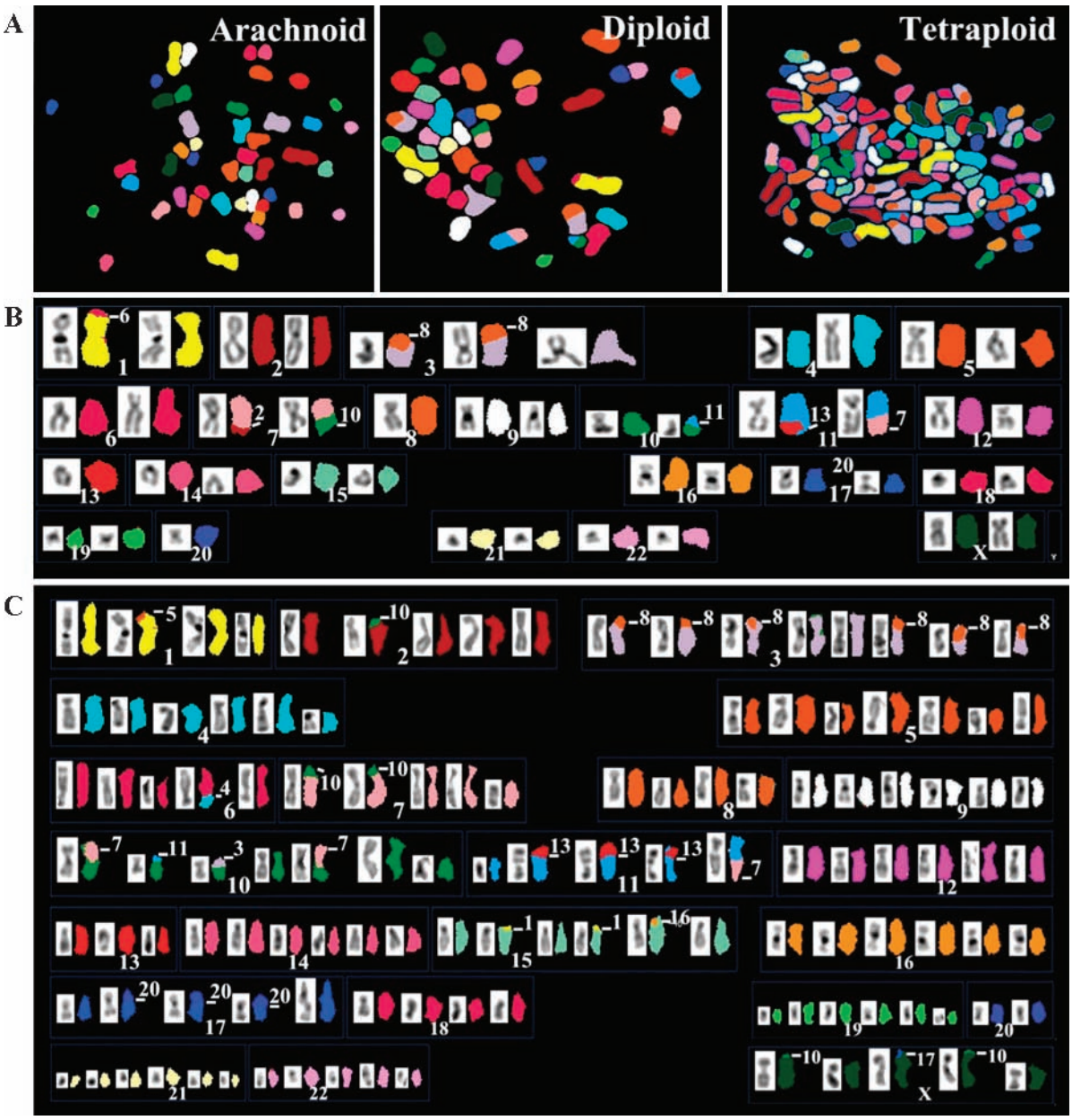

Figure 5. Tetraploid cells develop a higher number of numerical and structural chromosomal abnormalities over time in culture when compared with diploid cells. Spectral karyotyping (SKY) was used to assess numerical and structural abnormalities in SF3061-Vector and isolated diploid and tetraploid cells from SF3061-HES1 stable cell populations. (A) Representative SKY metaphases from control nonneoplastic arachnoid (Arachnoid) cells, SF3061-Vector (Diploid), and SF3061-HES1 (Tetraploid) cells are shown. (B and C) SKY karyograms of a diploid metaphase from SF3061-Vector cells at passage 19 (B) and a tetraploid metaphase from SF3061-HES1 cells at passage 19 (C) are shown. Chromosome numbers (white) are indicated.

Table 1. Numerical and Structural Chromosomal Abnormalities in SF3061 Meningioma Cells.

Stable Cell Population	Passage Number	Number of Metaphases Analyzed	Total Number of Translocations	Translocations per Metaphase	Mean Number of Chromosomes per Metaphase
SF3061-Vector	8	15	138	9.2	42.8
SF3061-HES1 Tetraploid	8	15	289	19.3	89.3
SF3061-Vector	19	15	141	9.4	42.9
SF3061-HES1 Tetraploid	19	15	426	28.4	117.6
SF3061-HES1 Diploid	19	8	71	8.9	42.3

clearly demonstrated in Barrett esophagus, a premalignant condition where patients are regularly followed by endoscopic biopsies [29,30]. A careful analysis of these patients has revealed the relatively early loss of p53, the acquisition of a significant population of tetraploid cells, and the subsequent development of aneuploidy. Also, in some tumor models, such as the elastase–simian virus 40 tumor antigen transgenic mouse model of pancreatic cancer, an increase in a tetraploid population of cells is detected early in the development of tumor [31].

Tetraploid cells are normally cell cycle–arrested and undergo apoptosis if there is an intact tetraploidy checkpoint [32]. Also, a disrupted p53 pathway has been proposed as being essential for the survival of tetraploid cells [32]. In our study, tetraploid meningioma cells associated with HES1 expression were viable albeit with a slightly elevated apoptotic rate suggesting that the meningioma cell lines used have a defective tetraploidy checkpoint. It is likely that any tetraploid cells generated by transfecting HES1 in untransformed cells that have robust cell cycle checkpoints would be eliminated.

In vivo, we anticipate that tetraploid meningioma cells without the ability to evade apoptosis will die. Only cells with another cellular defect such as a disrupted p53 pathway would survive. This could potentially occur through a "prior genetic hit" that has provided a growth advantage to the cell. A more likely scenario is that the genetically unstable tetraploid cell itself acquires a mutation or translocation that provides a selective growth advantage allowing it to propagate.

Previous studies have shown that primary meningioma tumors contain tetraploid cells and exhibit chromosomal instability. Fluorescence *in situ* hybridization studies aimed at investigating chromosomal aberrations in meningiomas have frequently detected tetraploid cells [33–35]. One study, investigating chromosome 14q32 loss in 124 meningiomas, found tetraploid cells in 26% of meningiomas [33]. Using flow cytometry, a hyperdiploid phenotype was observed in 30% (44/124 tumors) of meningioma cases analyzed [36]. In a separate study, specific features of chromosomal instability have also been found at high frequency in meningiomas [37]. Early passage short-term primary cultures from 61 meningiomas were analyzed and shown to have cells with aberrant nuclear morphology including multinucleated cells, anaphase bridges, chromatin strings and nuclear blebs [37]. Chromosomal aberrations including ring chromosomes, telomere associations, and dicentric chromosomes were observed. A hyperdiploid karyotype was found in 47.5% of these tumors. The authors concluded that even slow-growing tumors such as meningiomas display chromosomal instability [37]. Our studies suggest that deregulation of the Notch signaling pathway is a potential mechanism that is responsible for this phenotype.

Notch has previously been implicated in the control of ploidy under certain cellular contexts. In the endocycle, DNA replication is uncoupled from mitosis allowing cells to dramatically increase their DNA content above diploid values. *Drosophila* follicle cells divide mitotically and increase in number until mid-oogenesis when they exit the mitotic cycle and enter the endocycle. The Notch signaling pathway controls this mitotic/endocycle switch. Loss of Notch or Delta results in the failure of these cells to form endocycles [38,39]. Similarly, in humans, megakaryocytes are specialized precursors of platelets that are polyploid. The Notch signaling pathway has been implicated in the generation of these polyploid megakaryocytes, although the mechanism of Notch function in this process is not understood [40,41]. Finally, in *Caenorhabditis elegans*, a gain of function mutation in *glp1*, an ortholog of Notch, prevents primordial germ cells from making the mitosis to meiosis switch (equivalent to twice the "normal" DNA content) and leads to the overgrowth of primordial germ cells and the formation of germline tumors [42]. In human germ cell tumors (seminomas and carcinoma *in situ*), Notch2 and Notch4 are over-expressed, and it has been proposed that deregulation of Notch causes dysfunction of the mitotic to meiotic switch leading to abnormal chromosomal segregation and the generation of aneuploid cells [43]. Thus, one of the many functions of the Notch signaling pathway in certain cell types is the regulation of ploidy. Our data show that meningiomas are one such cell type.

Tetraploidy can be induced by external signals or mutations that result in either cell fusion or an abortive cell cycle including defects in DNA replication, sister chromatid separation, mitotic spindle assembly, mitotic checkpoint regulation, or cytokinesis [21,44]. The aberrant expression of proteins regulating the G_2/M phase transition such as Aurora A, cyclin B1, forkhead transcription factor M3, and mitotic spindle checkpoint proteins such as Bub and Mad have been shown to induce tetraploidy [45,46]. It is possible the Notch signaling induces tetraploidy by impacting expression of one or more of these proteins. Understanding the mechanism by which Notch signaling induces tetraploidy in meningiomas remains to be determined and will be an important topic of future work.

In conclusion, our data identify a function for Notch signaling in inducing chromosomal instability in meningiomas and potentially contributing to meningioma tumorigenesis.

Acknowledgments

The authors thank Lucio Miele and Spyros Artavanis-Tsakonas for providing expression constructs, Jingli Weier for assistance with Spectral Karyotyping analysis, Tetsuo Sudo for the HES1 antibody, and the UCSF Comprehensive Cancer Center LCA Core for technical assistance with the flow cytometric analysis. The authors also thank Katharine Striedinger and Lucia Carvalho for useful discussions and critical review of the manuscript. A. L. is a recipient of The Sontag Foundation Distinguished Scientist Award.

References

[1] Kopan R (2002). Notch: a membrane-bound transcription factor. *J Cell Sci* **115**, 1095–1097.

[2] Iso T, Kedes L, and Hamamori Y (2003). HES and HERP families: multiple effectors of the Notch signaling pathway. *J Cell Physiol* **194**, 237–255.

[3] Bolos V, Grego-Bessa J, and de la Pompa JL (2007). Notch signaling in development and cancer. *Endocr Rev* **28**, 339–363.

[4] Radtke F and Raj K (2003). The role of Notch in tumorigenesis: oncogene or tumour suppressor? *Nat Rev Cancer* **3**, 756–767.

[5] Capobianco AJ, Zagouras P, Blaumueller CM, Artavanis-Tsakonas S, and Bishop JM (1997). Neoplastic transformation by truncated alleles of human NOTCH1/TAN1 and NOTCH2. *Mol Cell Biol* **17**, 6265–6273.

[6] Pear WS, Aster JC, Scott ML, Hasserjian RP, Soffer B, Sklar J, and Baltimore D (1996). Exclusive development of T cell neoplasms in mice transplanted with bone marrow expressing activated Notch alleles. *J Exp Med* **183**, 2283–2291.

[7] Nicolas M, Wolfer A, Raj K, Kummer JA, Mill P, van Noort M, Hui CC, Clevers H, Dotto GP, and Radtke F (2003). Notch1 functions as a tumor suppressor in mouse skin. *Nat Genet* **33**, 416–421.

[8] Zagouras P, Stifani S, Blaumueller CM, Carcangiu ML, and Artavanis-Tsakonas S (1995). Alterations in Notch signaling in neoplastic lesions of the human cervix. *Proc Natl Acad Sci USA* **92**, 6414–6418.

[9] Talora C, Sgroi DC, Crum CP, and Dotto GP (2002). Specific down-modulation of Notch1 signaling in cervical cancer cells is required for sustained *HPV-E6/E7* expression and late steps of malignant transformation. *Genes Dev* **16**, 2252–2263.

[10] Zeng Q, Li S, Chepeha DB, Giordano TJ, Li J, Zhang H, Polverini PJ, Nor J, Kitajewski J, and Wang CY (2005). Crosstalk between tumor and endothelial cells promotes tumor angiogenesis by MAPK activation of Notch signaling. *Cancer Cell* **8**, 13–23.

[11] Cuevas IC, Slocum AL, Jun P, Costello JF, Bollen AW, Riggins GJ, McDermott MW, and Lal A (2005). Meningioma transcript profiles reveal deregulated notch signaling pathway. *Cancer Res* **65**, 5070–5075.

[12] CBTRUS (2005). *Statistical Report: Primary Brain Tumors in the United States, 1998–2002.* Hinsdale, IL: Central Brain Tumor Registry of the United States.

[13] Baser ME, R Evans DG, and Gutmann DH (2003). Neurofibromatosis 2. *Curr Opin Neurol* **16**, 27–33.

[14] Ringel F, Cedzich C, and Schramm J (2007). Microsurgical technique and results of a series of 63 spheno-orbital meningiomas. *Neurosurgery* **60**, 214–221 [discussion 221–212].

[15] Bassiouni H, Asgari S, and Stolke D (2007). Olfactory groove meningiomas: functional outcome in a series treated microsurgically. *Acta Neurochir (Wien)* **149**, 109–121 [discussion 121].

[16] Perry A, Scheithauer BW, Stafford SL, Lohse CM, and Wollan PC (1999). "Malignancy" in meningiomas: a clinicopathologic study of 116 patients, with grading implications. *Cancer* **85**, 2046–2056.

[17] Kepes JJ (1986). Presidential address: the histopathology of meningiomas. A reflection of origins and expected behavior? *J Neuropathol Exp Neurol* **45**, 95–107.

[18] O'Rahilly R and Muller F (1986). The meninges in human development. *J Neuropathol Exp Neurol* **45**, 588–608.

[19] Baia GS, Slocum AL, Hyer JD, Misra A, Sehati N, Vandenberg SR, Feuerstein BG, Deen DF, McDermott MW, and Lal A (2006). A genetic strategy to overcome the senescence of primary meningioma cell cultures. *J Neurooncol* **78**, 113–121.

[20] Fung J, Weier HU, Goldberg JD, and Pedersen RA (2000). Multilocus genetic analysis of single interphase cells by spectral imaging. *Hum Genet* **107**, 615–622.

[21] Storchova Z and Pellman D (2004). From polyploidy to aneuploidy, genome instability and cancer. *Nat Rev Mol Cell Biol* **5**, 45–54.

[22] Curry CL, Reed LL, Nickoloff BJ, Miele L, and Foreman KE (2006). Notch-independent regulation of Hes-1 expression by c-Jun N-terminal kinase signaling in human endothelial cells. *Lab Invest* **86**, 842–852.

[23] Fan X, Mikolaenko I, Elhassan I, Ni X, Wang Y, Ball D, Brat DJ, Perry A, and Eberhart CG (2004). Notch1 and Notch2 have opposite effects on embryonal brain tumor growth. *Cancer Res* **64**, 7787–7793.

[24] Tohda S, Kogoshi H, Murakami N, Sakano S, and Nara N (2005). Diverse effects of the Notch ligands Jagged1 and Delta1 on the growth and differentiation of primary acute myeloblastic leukemia cells. *Exp Hematol* **33**, 558–563.

[25] Castedo M, Coquelle A, Vivet S, Vitale I, Kauffmann A, Dessen P, Pequignot MO, Casares N, Valent A, Mouhamad S, et al. (2006). Apoptosis regulation in tetraploid cancer cells. *EMBO J* **25**, 2584–2595.

[26] Coursen JD, Bennett WP, Gollahon L, Shay JW, and Harris CC (1997). Genomic instability and telomerase activity in human bronchial epithelial cells during immortalization by human papillomavirus-16 *E6* and *E7* genes. *Exp Cell Res* **235**, 245–253.

[27] Takeuchi M, Takeuchi K, Kohara A, Satoh M, Shioda S, Ozawa Y, Ohtani A, Morita K, Hirano T, Terai M, et al. (2007). Chromosomal instability in human mesenchymal stem cells immortalized with human papilloma virus *E6*, *E7*, and *hTERT* genes. *In Vitro Cell Dev Biol Anim* **43**, 129–138.

[28] Olaharski AJ, Sotelo R, Solorza-Luna G, Gonsebatt ME, Guzman P, Mohar A, and Eastmond DA (2006). Tetraploidy and chromosomal instability are early events during cervical carcinogenesis. *Carcinogenesis* **27**, 337–343.

[29] Galipeau PC, Cowan DS, Sanchez CA, Barrett MT, Emond MJ, Levine DS, Rabinovitch PS, and Reid BJ (1996). 17p (p53) allelic losses, 4N (G_2/tetraploid) populations, and progression to aneuploidy in Barrett's esophagus. *Proc Natl Acad Sci USA* **93**, 7081–7084.

[30] Barrett MT, Pritchard D, Palanca-Wessels C, Anderson J, Reid BJ, and Rabinovitch PS (2003). Molecular phenotype of spontaneously arising 4N (G_2-tetraploid) intermediates of neoplastic progression in Barrett's esophagus. *Cancer Res* **63**, 4211–4217.

[31] Levine DS, Sanchez CA, Rabinovitch PS, and Reid BJ (1991). Formation of the tetraploid intermediate is associated with the development of cells with more than four centrioles in the elastase–simian virus 40 tumor antigen transgenic mouse model of pancreatic cancer. *Proc Natl Acad Sci USA* **88**, 6427–6431.

[32] Margolis RL, Lohez OD, and Andreassen PR (2003). G_1 tetraploidy checkpoint and the suppression of tumorigenesis. *J Cell Biochem* **88**, 673–683.

[33] Tabernero MD, Espinosa AB, Maillo A, Sayagues JM, Alguero Mdel C, Lumbreras E, Diaz P, Goncalves JM, Onzain I, Merino M, et al. (2005). Characterization of chromosome 14 abnormalities by interphase *in situ* hybridization and comparative genomic hybridization in 124 meningiomas: correlation with clinical, histopathologic, and prognostic features. *Am J Clin Pathol* **123**, 744–751.

[34] Maillo A, Diaz P, Sayagues JM, Blanco A, Tabernero MD, Ciudad J, Lopez A, Goncalves JM, and Orfao A (2001). Gains of chromosome 22 by fluorescence *in situ* hybridization in the context of an hyperdiploid karyotype are associated with aggressive clinical features in meningioma patients. *Cancer* **92**, 377–385.

[35] Sayagues JM, Tabernero MD, Maillo A, Diaz P, Rasillo A, Bortoluci A, Gomez-Moreta J, Santos-Briz A, Morales F, and Orfao A (2002). Incidence of numerical chromosome aberrations in meningioma tumors as revealed by fluorescence *in situ* hybridization using 10 chromosome-specific probes. *Cytometry* **50**, 153–159.

[36] Sayagues JM, Tabernero MD, Maillo A, Espinosa A, Rasillo A, Diaz P, Ciudad J, Lopez A, Merino M, Goncalves JM, et al. (2004). Intratumoral patterns of clonal evolution in meningiomas as defined by multicolor interphase fluorescence *in situ* hybridization (FISH): is there a relationship between histopathologically benign and atypical/anaplastic lesions? *J Mol Diagn* **6**, 316–325.

[37] van Tilborg AA, Al Allak B, Velthuizen SC, de Vries A, Kros JM, Avezaat CJ, de Klein A, Beverloo HB, and Zwarthoff EC (2005). Chromosomal instability in meningiomas. *J Neuropathol Exp Neurol* **64**, 312–322.

[38] Deng WM, Althauser C, and Ruohola-Baker H (2001). Notch-Delta signaling induces a transition from mitotic cell cycle to endocycle in *Drosophila* follicle cells. *Development* **128**, 4737–4746.

[39] Shcherbata HR, Althauser C, Findley SD, and Ruohola-Baker H (2004). The mitotic-to-endocycle switch in *Drosophila* follicle cells is executed by Notch-dependent regulation of G_1/S, G_2/M and M/G_1 cell-cycle transitions. *Development* **131**, 3169–3181.

[40] Sun L, Tan P, Yap C, Hwang W, Koh LP, Lim CK, and Aw SE (2004). *In vitro* biological characteristics of human cord blood–derived megakaryocytes. *Ann Acad Med Singapore* **33**, 570–575.

[41] Singh N, Phillips RA, Iscove NN, and Egan SE (2000). Expression of notch receptors, notch ligands, and fringe genes in hematopoiesis. *Exp Hematol* **28**, 527–534.

[42] Berry LW, Westlund B, and Schedl T (1997). Germ-line tumor formation caused by activation of *glp-1*, a *Caenorhabditis elegans* member of the Notch family of receptors. *Development* **124**, 925–936.

[43] Adamah DJ, Gokhale PJ, Eastwood DJ, Rajpert De-Meyts E, Goepel J, Walsh JR, Moore HD, and Andrews PW (2006). Dysfunction of the mitotic:meiotic switch as a potential cause of neoplastic conversion of primordial germ cells. *Int J Androl* **29**, 219–227.

[44] Nguyen HG and Ravid K (2006). Tetraploidy/aneuploidy and stem cells in cancer promotion: the role of chromosome passenger proteins. *J Cell Physiol* **208**, 12–22.

[45] Meraldi P, Draviam VM, and Sorger PK (2004). Timing and checkpoints in the regulation of mitotic progression. *Dev Cell* **7**, 45–60.

[46] Meraldi P, Honda R, and Nigg EA (2002). Aurora-A overexpression reveals tetraploidization as a major route to centrosome amplification in p53–/– cells. *EMBO J* **21**, 483–492.

IV- PUBLICAÇÕES

2- An orthotopic skull base model of malignant meningioma

Baia GS, Dinca EB, Ozawa T, Kimura ET,
McDermott MW, James CD, VandenBerg SR, Lal A

Brain Pathology, 18(2): 172-179, 2008

Brain Pathology ISSN 1015-6305

RESEARCH ARTICLE

An Orthotopic Skull Base Model of Malignant Meningioma

Gilson S. Baia[1]; Eduard B. Dinca[1]; Tomoko Ozawa[1]; Edna T. Kimura[2]; Michael W. McDermott[1]; C. David James[1]; Scott R. VandenBerg[1]; Anita Lal[1]

[1] Brain Tumor Research Center, Department of Neurological Surgery, University of California, San Francisco, CA 94143.
[2] Department of Cell and Developmental Biology, Institute of Biomedical Sciences, University of Sao Paulo, Sao Paulo, SP, Brazil.

Keywords
bioluminescent imaging, IOMM-Lee, meningioma, orthotopic, skull base, xenografts.

Corresponding author:
Anita Lal, PhD, Brain Tumor Research Center, Department of Neurological Surgery, Box 0520, University of California, San Francisco, CA 94143 (E-mail: *anita.lal@ucsf.edu*)

Received: 23 May 2007; revised 27 July 2007; accepted 4 September 2007.

doi:10.1111/j.1750-3639.2007.00109.x

Abstract

Meningioma tumor growth involves the subarachnoid space that contains the cerebrospinal fluid. Modeling tumor growth in this microenvironment has been associated with widespread leptomeningeal dissemination, which is uncharacteristic of human meningiomas. Consequently, survival times and tumor properties are varied, limiting their utility in testing experimental therapies. We report the development and characterization of a reproducible orthotopic skull-base meningioma model in athymic mice using the IOMM-Lee cell line. Localized tumor growth was obtained by using optimal cell densities and matrigel as the implantation medium. Survival times were within a narrow range of 17–21 days. The xenografts grew locally compressing surrounding brain tissue. These tumors had histopathologic characteristics of anaplastic meningiomas including high cellularity, nuclear pleomorphism, cellular pattern loss, necrosis and conspicuous mitosis. Similar to human meningiomas, considerable invasion of the dura and skull and some invasion of adjacent brain along perivascular tracts were observed. The pattern of hypoxia was also similar to human malignant meningiomas. We use bioluminescent imaging to non-invasively monitor the growth of the xenografts and determine the survival benefit from temozolomide treatment. Thus, we describe a malignant meningioma model system that will be useful for investigating the biology of meningiomas and for preclinical assessment of therapeutic agents.

INTRODUCTION

Meningiomas are common tumors of the central nervous system that originate from the meningeal covering (22), and therefore can occur in any location along the entire neural axis. They are a source of considerable morbidity and mortality because of their location and the existence of aggressive variants (18). Nevertheless, meningiomas remain a poorly understood cancer. A major obstacle to achieving an improved understanding of the molecular basis of meningioma tumorigenesis, and to evaluating experimental therapies for meningioma treatment, has been the scarcity of *in vitro* and *in vivo* model systems. Recently, considerable progress has been made in successfully growing meningioma cell lines *in vitro* (1, 20). These cell lines represent promising new tools for investigating the biology of meningiomas. However, *in vivo* meningioma model systems still have problems that restrict their utility (11, 16, 27).

Attempts at propagating available meningioma cell lines as orthotopic xenografts have been unable to recapitulate the human tumor growth pattern, as implantation of tumor cells results in widespread leptomeningeal dissemination throughout the subdural and intraventricular space (16, 27). Consequently, quantification of tumor growth as well as response to therapeutic agents is difficult compromising the utility of the model systems (16). The purpose of this study was to locally constrain meningioma tumor growth and develop a clinically relevant meningioma model system in athymic mice. Because skull base meningiomas are challenging to remove surgically and patients with these meningiomas have a worse prognosis (15, 17), we chose to develop a skull base model using the malignant meningioma cell line, IOMM-Lee, which is tumorigenic *in vivo* and grows at a rapid rate (13). By modifying these cells with a luciferase reporter, we have been able to additionally use bioluminescent imaging (BLI) to monitor *in vivo* growth of these cells, as well as their response to temozolomide therapy.

MATERIALS AND METHODS

Generation of enhanced green fluorescent protein and firefly luciferase expressing IOMM-Lee cells

The intraosseous malignant meningioma derived cell line, IOMM-Lee, was used in all the experiments described in this report (13, 14). IOMM-Lee cells were electroporated (Gene Pulser X Cell, Biorad, Hercules, CA, USA) with the enhanced green fluorescent protein (EGFP)-N3 plasmid (BD Biosciences, San Jose, CA, USA) and single clones expressing EGFP were selected in 600 μg/mL G418. IOMM-Lee cells were tagged with firefly luciferase (fluc) under the control of the spleen focus forming virus promoter using lentiviral-mediated gene transfer (9). Lentiviruses were generated

© 2007 The Authors; Journal Compilation © 2007 International Society of Neuropathology

by cotransfection of 293T cells with plasmids for gag-pol, env and fluc. The 48 h post-transfection filtered supernatant was used to infect IOMM-Lee cells.

Intracranial IOMM-Lee transplantations

All animal experiments were conducted following protocols approved by the University of California, San Francisco, Institutional Animal Care and Use Committee. Five- to six-week-old female athymic mice were anesthetized with Ketamine/Xylazine and fixed in a Model 940 stereotactic frame (David Kopf Instruments, Tujunga, CA, USA). The skull base region was reached by using the following injection coordinates: 2 mm to the right of the bregma, 2 mm posterior to the bregma and 5.8 mm below the skull surface. The indicated cell numbers and volumes of IOMM-Lee suspended in phosphate buffered saline (PBS) or matrigel were implanted using a Model 5000 Microinjection Unit (David Kopf Instruments, Tujunga, CA, USA) loaded with a 5 µL Hamilton 7105 syringe. For injection volumes of 0.5 µL, cells were steadily implanted over a period of 70 s and the needle was left in place for 1 minute before it was withdrawn slowly. The skull burr-hole was sealed with bone-wax and the skin incision was closed with 7 mm staples. Control mice were implanted with matrigel alone. The mice were monitored closely and were euthanized if they exhibited any neurological symptoms or had >15% weight loss or at predefined times post-implantation. The estimated survival times were the times from cell implantation to euthanasia.

Tissue processing and immunohistochemistry

EGFP fluorescence in tumor cells was analyzed in formalin fixed mouse heads after removal of the skull with a Leica MZ Fluo III stereomicroscope equipped with a Leica GFP-plus filter set. For histopathologic examination, mouse heads with the skull intact were fixed in 10% neutral buffered formalin for 48 h, decalcified in Decal Rapid Bone Decalcifier (American Histology, Lodi, CA, USA) for 24 h, and embedded in paraffin. Serial 10 µm thick sections were cut, numbered and processed for either hematoxylin and eosin (H&E) staining or immunohistochemistry. Immunohistochemistry was performed for vimentin using the clone Vim 3B4 antibody (1:100; Dako Corporation, Carpinteria, CA, USA), for carbonic anhydrase 9 (CA9) using the NB 100-417 antibody (1:1000; Novus Biologicals, Littleton, CO, USA) and for the Ki67 antigen using the clone MIB-1 antibody (1:100; Dako Corporation, Carpinteria, CA, USA) as described earlier (28). For calculating the MIB-labeling index, a total of 1000 nuclei in three hot-spots were counted.

BLI of luciferase—IOMM-Lee xenografts

BLI of intracranial xenografts was performed using the IVIS Lumina System (Xenogen Corp., Alameda, CA, USA) coupled to the data-acquisition LivingImage software (Xenogen Corp.). Before imaging, the mice were anesthetized with Ketamine/Xylazine. Thirty mg/mL of luciferin (potassium salt; Gold Biotechnology, St Louis, MO, USA) in PBS was injected intraperitoneally at a dose of 150 mg/kg body weight. Images were acquired between 10 and 20 minutes post-luciferin administration and peak luminescent signal was recorded. Signal intensity was quantitated as the sum of all detected photon counts within a region of interest using the LivingImage software package (6).

Temozolomide treatment and statistical analysis

For assaying *in vitro* sensitivity to temozolomide (TMZ), 100 000 IOMM-Lee and IOMM-Lee-Luc cells were plated in six well plates and the indicated concentration of TMZ was added at 24, 48 and 72 h. At 144 h, the cells were trypsinized, resuspended in 1 mL media and processed using the MTT Cell Proliferation Assay (ATCC, Manassas, VA, USA) following manufacturer's direction. Absorbance was read at 590 nm. The luminescence of IOMM-Lee-Luc cells treated with TMZ as described above was also read at 144 h in six well plates using the IVIS Lumina System in the presence of 30 µL of 30 mg/mL luciferin (potassium salt; Gold Biotechnology, St Louis, MO, USA). All *in vitro* experiments were performed in triplicate. For assaying *in vivo* sensitivity to TMZ, five mice bearing IOMM-Lee xenografts were orally administered with 120 mg/kg of TMZ for four consecutive days starting on day 10. Five mice bearing IOMM-Lee xenografts constituted the control group and received no treatment. The Kaplan-Meier estimator was used to generate the survival curves (12). Differences between survival curves were compared using a log-rank test (19).

Methylation-specific polymerase chain reaction (MSP)

Genomic DNA from IOMM-Lee cells was isolated using the DNeasy kit (Qiagen, Valencia, CA, USA). The methylation status of the O^6-methylguanine-DNA methyltransferase (MGMT) gene promoter was determined by MSP as described earlier (4, 7). Bisulfite treatment of isolated DNA was performed using the EZ DNA Methylation Gold kit (Zymo Research, Orange, CA, USA), followed by polymerase chain reaction (PCR) amplification to distinguish methylated and unmethylated DNA using PCR conditions and primers described earlier (7).

RESULTS

Fluorescent and bioluminescent tagging of IOMM-Lee cells

In order to accurately assess the extent of leptomeningeal dissemination, IOMM-Lee cells were fluorescently labeled with EGFP and a single high-level EGFP expressing clone, designated IOMM-Lee-EGFP2, was selected for further analysis. For BLI, IOMM-Lee cells were transduced with lentivirus encoding firefly luciferase, and transduced cell pools (IOMM-Lee-Luc) were injected in mice. IOMM-Lee-EGFP2, IOMM-Lee-Luc and parental IOMM-Lee had similar growth curves *in vitro* (data not shown). Also, IOMM-Lee-EGFP2 and parental IOMM-Lee had similar growth curves as subcutaneous tumors in athymic mice (data not shown). Thus, there was no indication of fluorescent and bioluminescent labeling altering the growth properties of IOMM-Lee parental cells.

Estimated survival times

We injected varying amounts and concentrations of IOMM-Lee-EGFP2 cells in PBS or matrigel into the skull base region of

© 2007 The Authors; Journal Compilation © 2007 International Society of Neuropathology

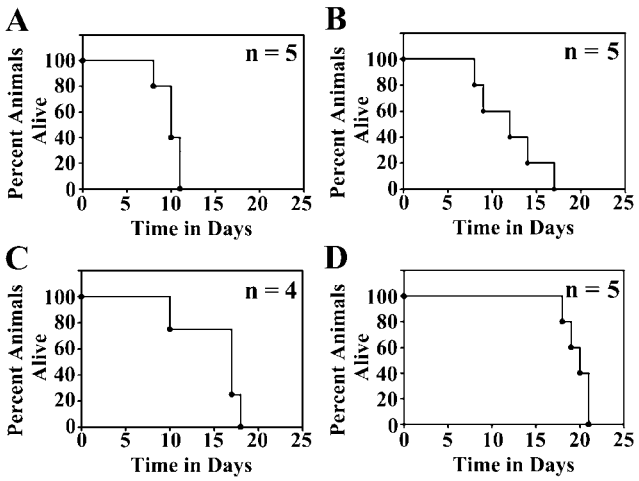

Figure 1. Estimated survival curves of athymic mice implanted with IOMM-Lee-EGFP2 cells in the skull base region. Athymic mice implanted with 3 000 000 cells/3 µL (**A**), 500 000 cells/5 µL (**B**), 50 000 cells/1 µL (**C**) or 50 000 cells/0.5 µL (**D**) were euthanized when they exhibited neurological symptoms or weight loss. Kaplan Meier plots for each implantation condition and the numbers of mice (n) in each group are shown.

athymic mice and calculated estimated survival times based on the appearance of neurological symptoms or weight loss. All the mice injected with IOMM-Lee-EGFP2 cells developed tumors. Thus, the tumor take rate with this cell line is 100%. Considerable variability in survival times and widespread leptomeningeal dissemination throughout the skull base and subarachnoid space was observed when PBS was used as an implantation medium (data not shown). When matrigel was used as an implantation medium, both intra- and inter-group variability in survival times were observed, with the extent of the former depending on both cell number and cell volume injected (Figure 1). For example, mice injected with 500 000 cells/5.0 µL died as early as 8 days or as late as 17 days (Figure 1), and this variability was caused by differences in tumor cell dissemination between mice receiving this amount and concentration of cells (data not shown). More consistent survival times with mice dying within 5 days of each other was observed for injections of 3 million cells/3.0 µL and 50 000 cells/0.5 µL (Figure 1). Of these two conditions, mice injected using the latter condition had slightly longer estimated survival times of 17–21 days and were chosen for use in subsequent investigations (see below).

Localized meningioma tumor growth

Macroscopic analysis of IOMM-Lee-EGFP2 xenograft growth revealed that the tumor mass did not invade the surface of the brain, and typically adhered to periosteal membranes when the skull and brain were separated (Figure 2). Examination of EGFP fluorescence revealed that tumor growth was confined to the site of implantation with minimal tumor cell dissemination to surrounding locations (Figure 2). The brain was visibly compressed at the location of the tumor.

Histopathology of IOMM-Lee xenografts

Histopathologic analyses were performed on tumors that were fixed, processed and sectioned *in situ* with the skull and brain intact. Xenografts displayed histopathologic features that were reminiscent of human anaplastic meningiomas, and included high cellularity, prominent nuclear pleomorphism marked by a high

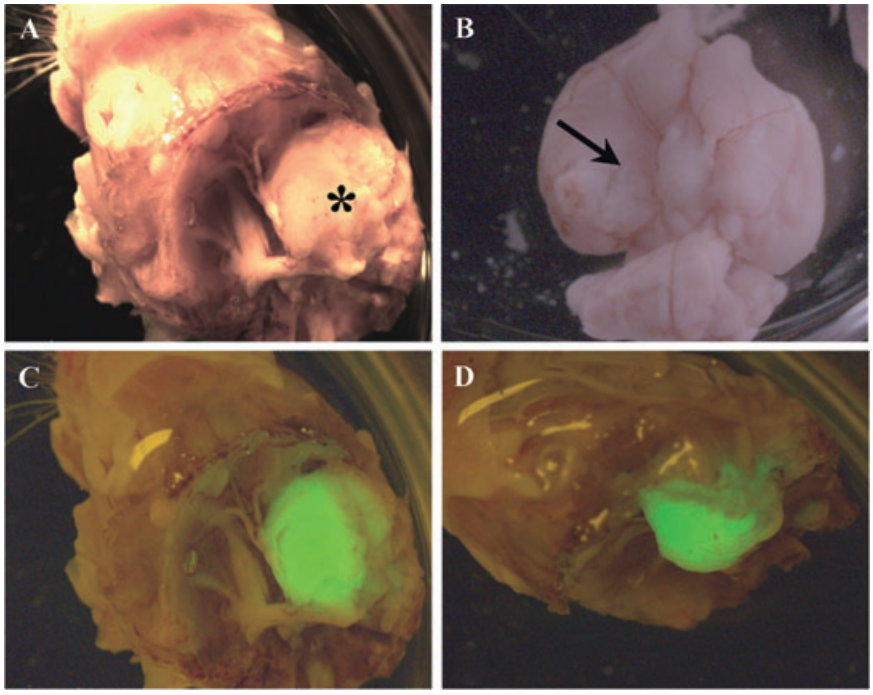

Figure 2. Macroscopic view of IOMM-Lee skull base meningioma xenografts. IOMM-Lee-EGFP2 cells were implanted in the skull base region using matrigel as the implantation medium to obtain localized tumor growth. The tumor mass (asterisk in **A**) was observed between the brain and the skull, and adhered to the skull when the skull (**A**) and brain (**B**) were separated. Compression of the brain was observed (arrow in **B**). Minimal leptomeningeal dissemination was observed as assessed by the distribution of the fluorescent EGFP label (**C**,**D**).

© 2007 The Authors; Journal Compilation © 2007 International Society of Neuropathology

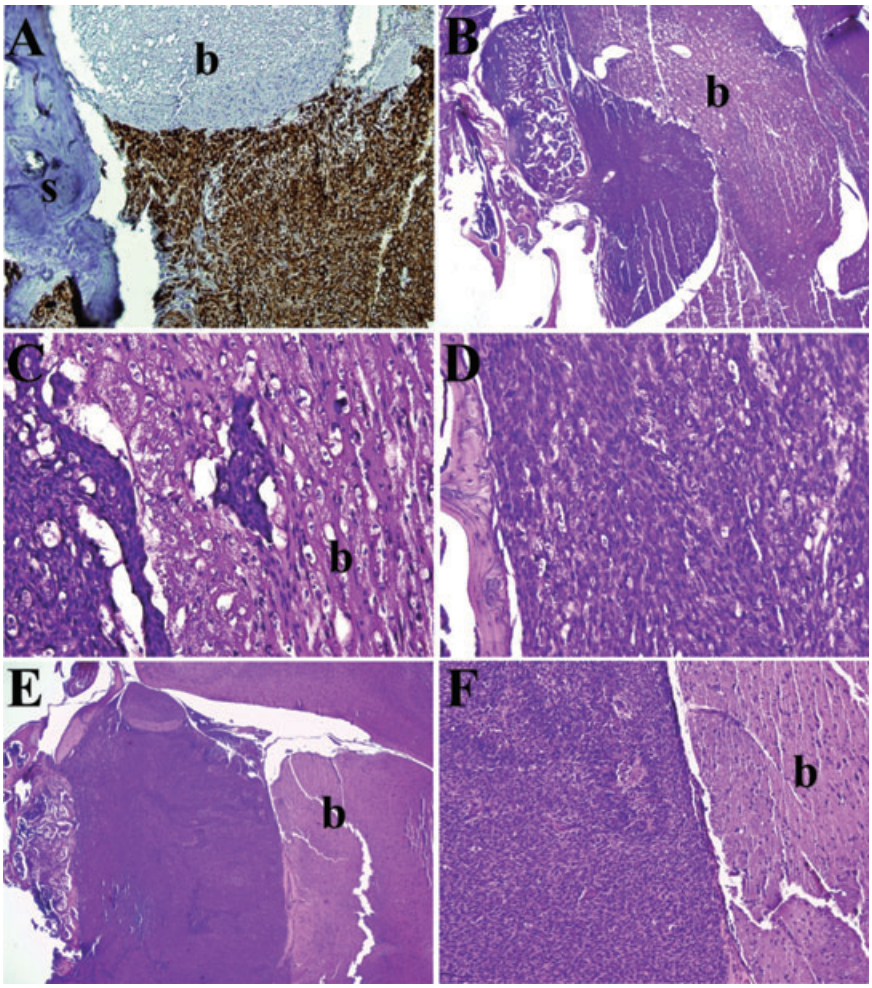

Figure 3. Growth Characteristics of IOMM-Lee skull base xenografts. Tissue sections of IOMM-Lee xenografts on day 6 (**A**), day 9 (**B**–**D**) and day 12 (**E**,**F**) were stained with human vimentin (**A**) or hematoxylin and eosin (**B–F**) and examined to evaluate the pattern of tumor growth. IOMM-Lee tumor growth maintained a well-demarcated boundary with the brain, except for microinvasion of the brain by small clumps of tumor cells (**C**). s, skull; b, brain.

nuclear to cytoplasmic ratio and prominent nucleoli. Cells were typically arranged in syncytial-like, highly cellular sheets with variable amounts of micro and geographic necrosis. Mitotic figures were conspicuous and the MIB-1 labeling indices were typically 30%.

Growth characteristics of IOMM-Lee xenografts

To evaluate xenograft growth patterns, brains with intact skulls were resected from mice injected with IOMM-Lee-Luc cells (50 000/0.5 μL) and sacrificed at days 3, 6, 9, 12, 16 post-implantation or when they exhibited weight loss and/or neurological symptoms. Fixed and embedded brain and skull tissue was serially sectioned, and examined by conventional H&E analysis or after staining for human vimentin. Progressive tumor growth was evident from day 3 onward, and by day 6, the tumor appeared to erode into the adjacent skull while primarily compressing the brain with early multifocal invasion into perivascular spaces (Figure 3). As the tumor mass enlarged, the boundary with the brain remained well-demarcated except for regions of microinvasion (Figures 3 and 4). By day 12 the xenografts had conspicuous necrotic zones, and the tumors had breached the pia and were invading the brain along perivascular and cranial nerve tracts (Figure 4). Immunohistochemical staining for human vimentin gave no indication of tumor dissemination at locations distant from the site of tumor implantation, and therefore meningioma tumor growth was localized to the site of tumor implantation.

Tumor hypoxia is an endogenous characteristic of malignant meningiomas, is associated with higher-grade histology as well as aggressive clinical behavior (28). With respect to this animal model of malignant meningioma, we assessed the appearance and prevalence of hypoxia by CA9 immunohistochemistry (28). Regions of hypoxia were first visible in day 9 xenografts (Figure 5), prior to the appearance of necrosis. Extensive hypoxic cell numbers were observed at the brain interface suggesting that this edge of the tumor was slower at recruiting vessels from the neuropil as opposed to non-brain interface tissue. Necrosis was first observed in day 12 tumors (Figure 5), and similar to human meningiomas, CA9 staining was zonal, found in viable cells surrounding regions of necrosis and also in regions not associated with any visible necrosis.

BLI of meningioma tumor burden

BLI was used to quantitate intracranial meningioma tumor growth rates in advance of testing tumor response to alkylator therapy.

© 2007 The Authors; Journal Compilation © 2007 International Society of Neuropathology

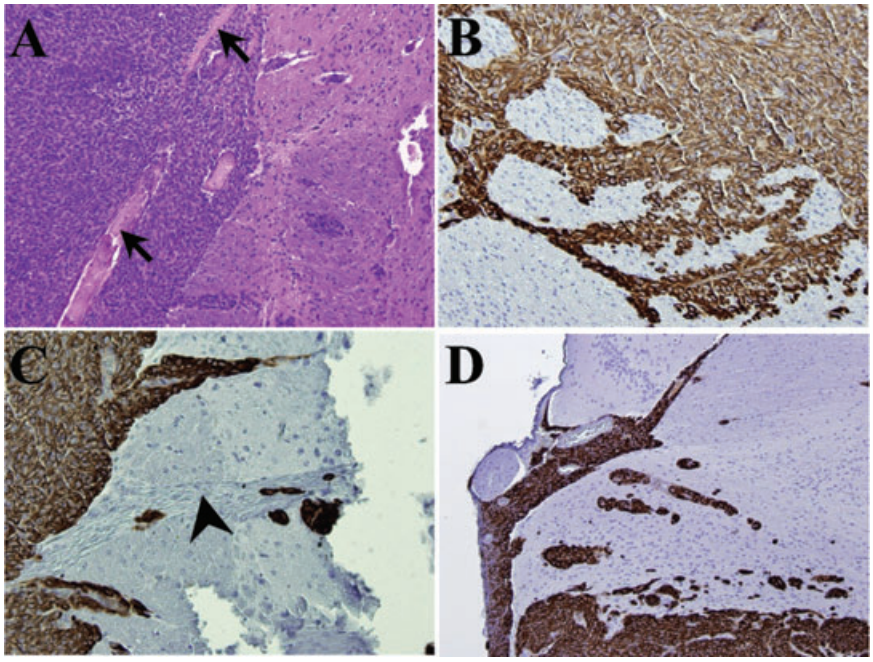

Figure 4. Pattern of brain invasion by IOMM-Lee xenografts. Tissue sections of IOMM-Lee xenografts on day 12 (**A–C**) or day 16 (**D**) were stained with human vimentin (**B–D**) or hematoxylin and eosin (**A**) and examined to evaluate the pattern of invasion of brain. By day 12, the tumor had breached the pia (**A**) and was invading the brain along perivascular (B) and cranial nerve (**C**) tracts. A similar pattern of invasion was observed in day 16 tumors (**D**). Arrow, pia; arrowhead, cranial nerve.

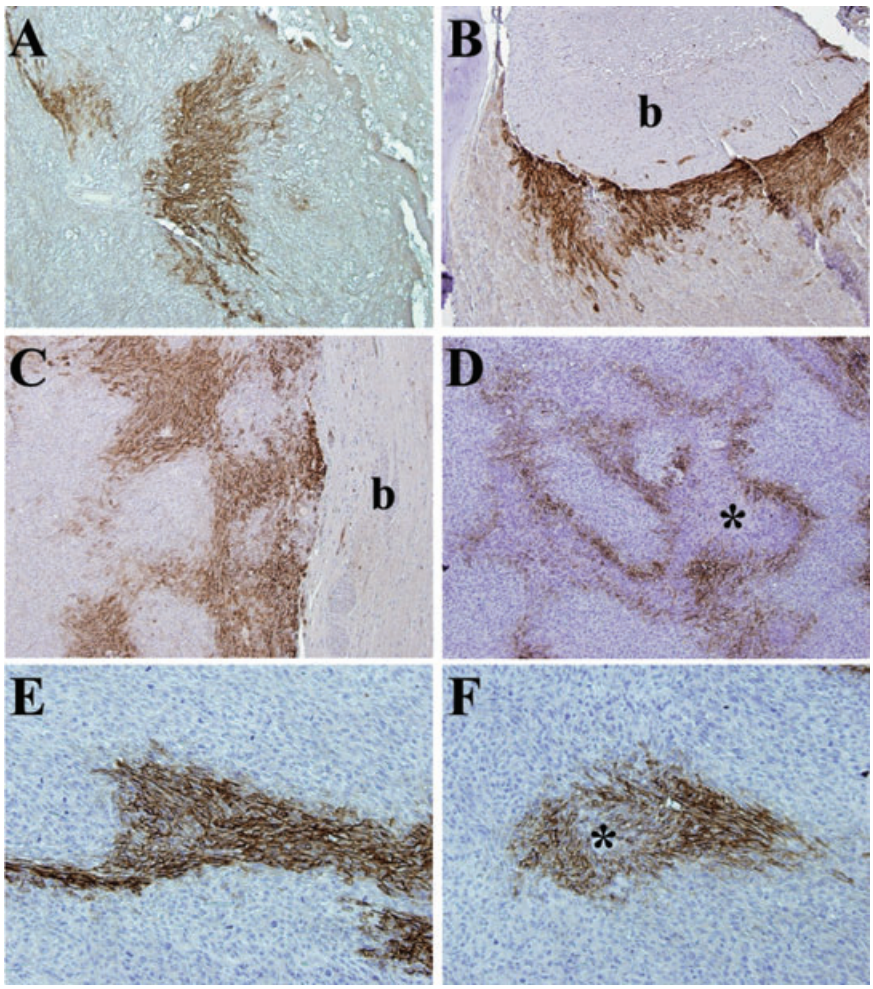

Figure 5. Pattern of hypoxia in IOMM-Lee skull-base xenografts. Immunohistochemistry with a polyclonal antibody against carbonic anhydrase 9 (CA9) was performed to evaluate the prevalence and distribution of hypoxia in tissue sections of IOMM-Lee xenografts on day 9 (**A**), day 12 (**B**), day 16 (**C**) and day 21 (**D–F**) post-implantation. Similar to human meningiomas, CA9 expression was zonal and sometimes not associated with any visible necrosis (**E**). The brain interface had considerable hypoxia (**B**,**C**) compared with the skull interface. b, brain; *, necrosis.

© 2007 The Authors; Journal Compilation © 2007 International Society of Neuropathology

Luminescence readings were detectable as early as day 3, and growth curves displayed consistent patterns of exponential increase between mice. Mice exhibited weight loss and neurological symptoms when photon counts of $3–4 \times 10^7$ were reached. In total, the BLI results showed reproducible growth of skull base xenografts, and provided pilot data for use in timing the administration of therapy in the subsequent experiment.

Xenograft response to TMZ therapy

To assess the efficacy of alkylator therapy, we treated IOMM-Lee and IOMM-Lee-Luc cells in culture with TMZ (Figure 6A,B). IOMM-Lee was sensitive to TMZ *in vitro* and the bioluminescent labeling did not alter the sensitivity to TMZ. Sensitivity to TMZ has been associated with *MGMT* promoter hypermethylation, and the *MGMT* promoter was methylated in IOMM-Lee cells (Figure 6C). To assess the *in vivo* sensitivity of IOMM-Lee xenografts to TMZ, tumor growth in control and TMZ-treated mice were followed using BLI. TMZ treatment resulted in a significant survival benefit to the mice (Figure 6, $P = 0.003$). While control group mice died by 17–21 days, one TMZ-treated mouse died on day 38 and the remaining four were still alive on day 43. To plot BLI tumor growth curves, each mouse's luminescence measurements were normalized against their own day 10 luminescence reading, allowing each mouse to serve as its own control. TMZ treatment arrested the rapid, exponential growth of the xenografts and resulted in reduced normalized luminescence readings (Figure 7). Recovery of exponential tumor growth was observed in the TMZ-treated mouse that died on day 38, while the remaining four mice had stable luminescent measurements till day 43 (Figure 7).

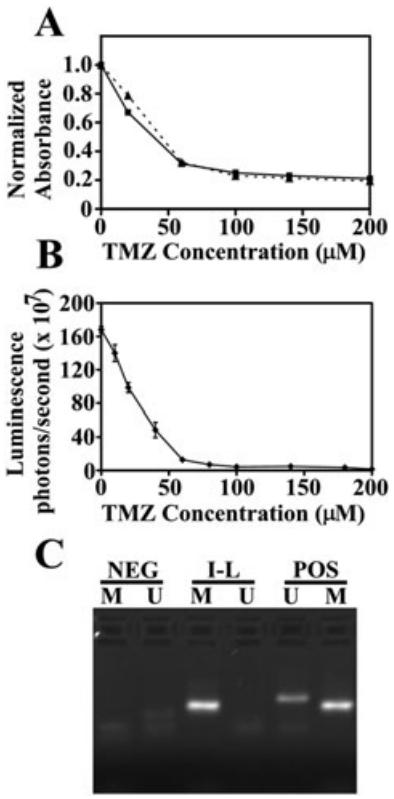

Figure 6. Efficacy of temozolomide (TMZ) in cultured IOMM-Lee cells and methylation status of the *O⁶-methylguanine-DNA methyltransferase (MGMT)* promoter. **A.** IOMM-Lee (squares and solid line) or IOMM-Lee-Luc cells (triangles and dashed line) were treated with the indicated concentration of TMZ and the number of viable cells was calculated using the MTT Cell Proliferation assay. Absorbance values were normalized to the no treatment control and plotted against TMZ concentration. The number of viable cells at different TMZ concentrations was similar for IOMM-Lee and IOMM-Lee-Luc cells. **B.** IOMM-Lee-Luc cells in culture were treated with the indicated concentration of TMZ and luminescence was measured at 144 h. Luminescence readings are plotted against TMZ concentration. **C.** Methylation-specific polymerase chain reaction was performed to determine the methylation status of the *MGMT* gene. The presence of a visible polymerase chain reaction product in the lane U indicates the presence of unmethylated *MGMT* gene and the presence of product in the lane M indicates the presence of methylated *MGMT* gene. *MGMT* is methylated in IOMM-Lee. Abbreviations: NEG = negative controls; I-L = IOMM-Lee; POS = positive controls.

DISCUSSION

Animal models are essential preclinical tools in the study of the molecular mechanisms of cancer and for evaluating anti-tumor therapies. A small number of meningioma animal models exist but every one of these systems has issues that limit their utility and/or clinical relevance. For example, in the genetic model of meningiomas, which is based on the knockout of the *NF2* gene specifically in arachnoidal cells, only 20% of the mice develop tumors after 11 to 14 months (11). Other model systems have utilized non-orthotopic locations that do not take micro-environmental influences of tumor growth into consideration. Rodent studies on the chemotherapeutic agent, hydroxyurea, were performed using meningioma cells grown in the galea (25), and tests on celecoxib were performed in subcutaneous tumors (21). Orthotopic meningioma model systems utilizing primary and established meningioma cell lines have been described (16, 27). However, primary meningioma cell lines senesce after a few passages and therefore these model systems are not reproducible (16, 27). Orthotopic models with established meningioma cell lines have been associated with widespread leptomeningeal dissemination limiting the ability to quantitate the extent of tumor growth in these systems.

In this study, we present a well-characterized, reproducible, clinically relevant skull base malignant meningioma xenograft model system in which we have overcome the problem of leptomeningeal dissemination. We show that localized meningioma tumor growth is sensitive to particular cell densities and is dependent on using matrigel as the implantation agent. In addition, we show that mice bearing localized xenografts had reproducible survival times within a range of 5 days. IOMM-Lee has been extensively used in meningioma research (23, 26) and has previously been implanted into the skull base region of mice (16, 27). However, localized tumor growth using this cell line has not previously been attained. Prior studies utilized PBS as the implantation agent, and it is likely that the use of matrigel would have reduced observed tumor cell dissemination. Previous reports of survival times with mice bearing IOMM-Lee orthotopic xenografts were similar to the survival times in this study (16, 24).

© 2007 The Authors; Journal Compilation © 2007 International Society of Neuropathology

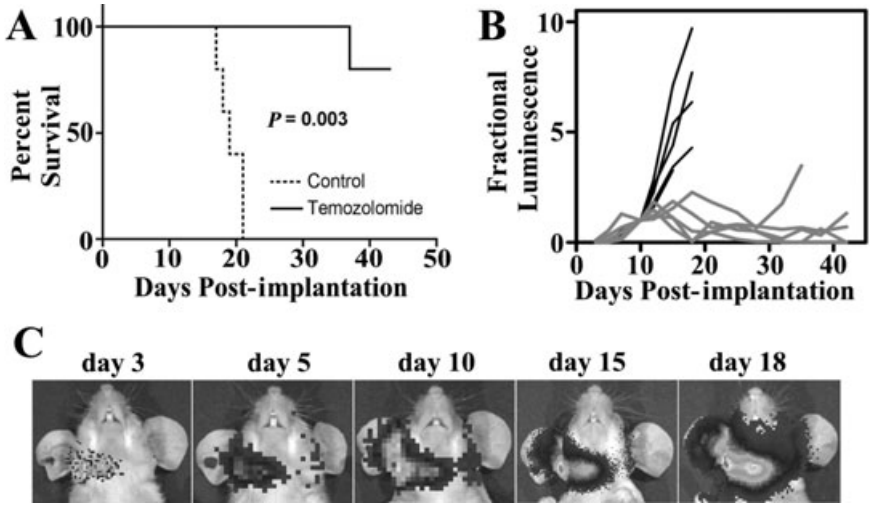

Figure 7. Bioluminescent imaging of IOMM-Lee xenografts, and their response to temozolomide (TMZ). Ten mice received injections of IOMM-Lee-Luc cells and were randomized into two groups that received either no treatment or treatment with 120 mg/kg TMZ for four consecutive days. **A.** Survival curves of athymic mice from control (dotted line) and TMZ-treatment (solid line) groups are plotted. A significant survival benefit ($P = 0.003$) for mice treated with TMZ was observed. **B.** Luminescence readings for each mouse were normalized against its own day 10 luminescence reading. Normalized BLI plots associated with monitoring of intracranial tumor growth for control (black line) and TMZ-treatment (gray line) groups are shown. **C.** Representative images from one control group mouse at the indicated time points post-implantation of IOMM-Lee-Luc cells are shown.

Preclinical cancer models should ideally resemble the human disease and mimic human tumor-host interactions. Human meningiomas are generally well-demarcated lesions that remain spherical or globular even after they attain considerable size (3). Consistent with the growth pattern of human meningiomas, IOMM-Lee xenografts grew as well-demarcated lesions between the skull and brain and remained globular even when the tumor mass was large. Malignant meningiomas commonly penetrate dura and invade bone. IOMM-Lee xenografts adhere to the skull and exhibit considerable invasion of the skull. Considerable compression of the brain was also observed. Human meningiomas grow as separate entities adjacent to the brain but often insinuate themselves into the subjacent cortex as small tongues or pegs of neoplastic tissue that follow the course of superficial blood vessels (3). IOMM-Lee xenografts followed a similar pattern of brain invasion, with small cell clumps invading the surrounding brain along perivascular and cranial nerve tracts.

Tumor hypoxia is significantly associated with higher histopathologic grade in meningiomas and is indicative of an aggressive meningioma phenotype (28). Similar to human meningiomas, the pattern of hypoxia in IOMM-Lee xenografts was found in the classic perinecrotic pattern in larger tumors with visible necrosis. Additionally, as in human meningiomas, hypoxia was found in histologically viable regions of tumors not associated with any visible necrosis. Interestingly, the amount of hypoxia at the brain interface was considerably greater than that at the skull interface, suggesting that the skull interface had easier access to a vascular supply. While the contribution of tumor hypoxia to meningioma growth is unknown, the current model system will allow such investigations and also allow testing of therapeutic strategies that target both normoxic and hypoxic cells.

BLI is an extremely accurate predictor of intracranial tumor burden and it has recently been shown using intracranial glioblastoma xenografts that there is an excellent correlation between intracranial tumor photon emission and tumor volume (6). BLI tumor growth curves for the IOMM-Lee xenografts were consistent between mice and BLI could accurately predict survival. Thus, BLI is ideal for following intracranial meningioma tumor growth and for monitoring therapeutic response. Meningioma tumor growth in animals has previously been monitored using contrast enhanced magnetic resonance imaging (MRI) (27). While MRI accurately follows tumor growth, it is a less cost–effective technique and relatively few researchers have access to such a facility. Immortalized benign meningioma cell lines have recently been developed in several laboratories (5, 20). These cell lines grow very slowly in mice and require long *in vivo* observation periods of several months. It is anticipated that BLI will be especially useful in following the tumor growth and monitoring the therapeutic response of these slower growing but more common meningiomas.

TMZ, a DNA methylating agent, has schedule-dependent antitumor activity against a variety of malignancies, including gliomas and melanomas (8). Currently, it is routinely used in the clinic to treat malignant gliomas. The efficacy of TMZ against malignant meningiomas has not been evaluated. In the current study, we show that TMZ was an effective therapy against rodent IOMM-Lee xenografts and resulted in a considerable survival benefit. Methylation of the promoter of the DNA-repair gene, *MGMT*, has been associated with sensitivity to TMZ in glioblastoma patients (10). The *MGMT* promoter was methylated in IOMM-Lee cells. Sixteen percent of all meningiomas have aberrant methylation of the *MGMT* promoter (2) and patients bearing these tumors could possibly respond to TMZ therapy. However, more detailed preclinical

© 2007 The Authors; Journal Compilation © 2007 International Society of Neuropathology

studies using this chemotherapeutic agent are necessary before conclusions on the effectiveness of TMZ as a therapeutic agent for meningiomas are made.

In summary, we have developed a rodent preclinical meningioma model system and show that it can be used to evaluate therapeutic regimens. This system has several features that mimic the human meningioma growth pattern and will enable us to dissect the biology of meningioma tumorigenesis, evaluate tumor-host interactions unique to meningiomas and test the toxicity and efficacy of novel therapeutic approaches.

ACKNOWLEDGMENTS

We thank Cynthia Cowdrey for technical assistance with tissue processing, Lily Hu for technical assistance with generation of the luciferase lentivirus, Jennifer Ayers-Ringler for technical assistance with the *MGMT* promoter methylation assay and Drs Katharine Striedinger and Jeanette Hyer for useful discussions and review of the manuscript. This study was supported by NIH/NINDS grant 1R03NS054829-01 to AL and SPORE grant P50CA097257 to CDJ.

REFERENCES

1. Baia GS, Slocum AL, Hyer JD, Misra A, Sehati N, Vandenberg SR *et al* (2006) A genetic strategy to overcome the senescence of primary meningioma cell cultures. *J Neurooncol* **78**:113–121.
2. Bello MJ, Aminoso C, Lopez-Marin I, Arjona D, Gonzalez-Gomez P, Alonso ME *et al* (2004) DNA methylation of multiple promoter-associated CpG islands in meningiomas: relationship with the allelic status at 1p and 22q. *Acta Neuropathol (Berl)* **108**:413–421.
3. Burger PC, Scheithauer BW, Vogel FS (2002) *Surgical Pathology of the Nervous System and Its Coverings*, 4th edn. Churchill Livingstone: New York.
4. Cankovic M, Mikkelsen T, Rosenblum ML, Zarbo RJ (2007) A simplified laboratory validated assay for MGMT promoter hypermethylation analysis of glioma specimens from formalin-fixed paraffin-embedded tissue. *Lab Invest* **87**:392–397.
5. Cargioli TG, Ugur HC, Ramakrishna N, Chan J, Black PM, Carroll RS (2007) Establishment of an in vivo meningioma model with human telomerase reverse transcriptase. *Neurosurgery* **60**:750–759; discussion 759–760.
6. Dinca EB, Sarkaria JN, Schroeder MA, Carlson BL, Voicu R, Berger MS, James CD (2007) Bioluminescence monitoring of intracranial gliolastoma xenograft response to primary and salvage temozolomide therapy. *J Neurosurg* **107**:610–616.
7. Esteller M, Hamilton SR, Burger PC, Baylin SB, Herman JG (1999) Inactivation of the DNA repair gene O6-methylguanine-DNA methyltransferase by promoter hypermethylation is a common event in primary human neoplasia. *Cancer Res* **59**:793–797.
8. Friedman HS, Kerby T, Calvert H (2000) Temozolomide and treatment of malignant glioma. *Clin Cancer Res* **6**:2585–2597.
9. Hasegawa K, Pham L, O'Connor MK, Federspiel MJ, Russell SJ, Peng KW (2006) Dual therapy of ovarian cancer using measles viruses expressing carcinoembryonic antigen and sodium iodide symporter. *Clin Cancer Res* **12**:1868–1875.
10. Hegi ME, Diserens AC, Gorlia T, Hamou MF, de Tribolet N, Weller M *et al* (2005) MGMT gene silencing and benefit from temozolomide in glioblastoma. *N Engl J Med* **352**:997–1003.
11. Kalamarides M, Niwa-Kawakita M, Leblois H, Abramowski V, Perricaudet M, Janin A *et al* (2002) Nf2 gene inactivation in arachnoidal cells is rate-limiting for meningioma development in the mouse. *Genes Dev* **16**:1060–1065.
12. Kaplan EL, Meier P (1958) Non-parametric estimation from incomplete observations. *J Am Stat Assoc* **53**:457–481.
13. Lee WH (1990) Characterization of a newly established malignant meningioma cell line of the human brain: IOMM-Lee. *Neurosurgery* **27**:389–395.
14. Lee WH, Tu YC, Liu MY (1988) Primary intraosseous malignant meningioma of the skull: case report. *Neurosurgery* **23**:505–508.
15. Mathiesen T, Lindquist C, Kihlstrom L, Karlsson B (1996) Recurrence of cranial base meningiomas. *Neurosurgery* **39**: 2–7.
16. McCutcheon IE, Friend KE, Gerdes TM, Zhang BM, Wildrick DM, Fuller GN (2000) Intracranial injection of human meningioma cells in athymic mice: an orthotopic model for meningioma growth. *J Neurosurg* **92**:306–314.
17. Mendenhall WM, Morris CG, Amdur RJ, Foote KD, Friedman WA (2003) Radiotherapy alone or after subtotal resection for benign skull base meningiomas. *Cancer* **98**:1473–1482.
18. Modha A, Gutin PH (2005) Diagnosis and treatment of atypical and anaplastic meningiomas: a review. *Neurosurgery* **57**:538–550.
19. Peto R, Peto J (1972) Asymptotically efficient rank invariant procedures. *J R Stat Soc Ser A Stat Soc* **135**:185–207.
20. Puttmann S, Senner V, Braune S, Hillmann B, Exeler R, Rickert CH, Paulus W (2005) Establishment of a benign meningioma cell line by hTERT-mediated immortalization. *Lab Invest* **85**:1163–1171.
21. Ragel BT, Jensen RL, Gillespie DL, Prescott SM, Couldwell WT (2006) Celecoxib inhibits meningioma tumor growth in a mouse xenograft model. *Cancer* **109**:588–597.
22. Riemenschneider MJ, Perry A, Reifenberger G (2006) Histological classification and molecular genetics of meningiomas. *Lancet Neurol* **5**:1045–1054.
23. Robb VA, Li W, Gutmann DH (2004) Disruption of 14-3-3 binding does not impair Protein 4.1B growth suppression. *Oncogene* **23**:3589–3596.
24. Salhia B, Rutka JT, Lingwood C, Nutikka A, Van Furth WR (2002) The treatment of malignant meningioma with verotoxin. *Neoplasia* **4**:304–311.
25. Schrell UM, Rittig MG, Anders M, Kiesewetter F, Marschalek R, Koch UH, Fahlbusch R (1997) Hydroxyurea for treatment of unresectable and recurrent meningiomas. I. Inhibition of primary human meningioma cells in culture and in meningioma transplants by induction of the apoptotic pathway. *J Neurosurg* **86**:845–852.
26. Surace EI, Lusis E, Haipek CA, Gutmann DH (2004) Functional significance of S6K overexpression in meningioma progression. *Ann Neurol* **56**:295–298.
27. van Furth WR, Laughlin S, Taylor MD, Salhia B, Mainprize T, Henkelman M *et al* (2003) Imaging of murine brain tumors using a 1.5 Tesla clinical MRI system. *Can J Neurol Sci* **30**:326–332.
28. Yoo H, Baia GS, Smith JS, McDermott MW, Bollen AW, Vandenberg SR *et al* (2007) Expression of the hypoxia marker carbonic anhydrase 9 is associated with anaplastic phenotypes in meningiomas. *Clin Cancer Res* **13**:68–75.

© 2007 The Authors; Journal Compilation © 2007 International Society of Neuropathology

V- CONCLUSÕES

1- A ativação de componentes da cascata de sinalização de Notch em meningiomas caracteriza-se pelo favorecimento à formação de células com ploidia nuclear alterada.

Uma vez isoladas, as células tetraplóides desmonstraram-se viáveis em cultura e exibem características de instabilidade genética, como: aumento da freqüência de figuras atípicas nucleares, pela presença de mitoses com fusos multipolares e de células com núcleos de tamanho aumentado.

Em comparação às células diplóides, as células tetraplóides apresentam maior taxa de espontânea de apoptose e desenvolvem uma taxa mais elevada de alterações cromossômicas estruturais e numéricas.

Desta forma, inferimos que a ativação da sinalização de Notch deve ser um mecanismo genético inicial no desenvolvimento de meningiomas, e potencialmente contribui para a tumorigênese.

2- Desenvolveu-se com sucesso um modelo ortotópico reprodutível de meningioma em camundongo atímico, que demonstrou ter utilidade para avaliação de tratamentos terapêuticos. O modelo apresenta ainda características histológicas e o padrão de crescimento que recapitulam o meningioma maligno humano e deverá ser útil para o entendimento futuro da biologia da doença.

A possibilidade do uso da técnica de bioluminescência permitiu o uso de menor número de animais nos experimentos, bem como possibilitou a mensuração *in vivo* do crescimento do tumor após a implantação das células. Observou-se ainda uma correlação positiva entre a bioluminescência medida e o tamanho do tumor.

Embora o emprego de temozolamida, como opção de terapêutica de meningiomas humanos necessite estudos mais detalhados, o tratamento dos animais implantados com temozolamida demonstrou um considerável benefício de sobrevivência aos animais. Portanto este modelo animal tem potencial utilidade para avaliação da eficácia de outras terapias para meningiomas.

VI- REFERÊNCIAS BIBLIOGRÁFICAS

Adamah DJ, Gokhale PJ, Eastwood DJ, Rajpert De-Myts E, Goepel J, Walsh JR, Moore HD, Andrews PW (2006). Dysfunction of the mitotic:meiotic switch as a potential cause of neoplastic conversion of primordial germ cells. **International Journal of Andrology, 29:219-227**.

Al-Mefty O, Kadri PA, Pravdenkova S, Sawyer JR, Stangeby C, Husain M (2004) Malignant progression in meningioma: documentation of a series and analysis of cytogenetic findings. **Journal of Neurosurgery, 101:210-218**.

Baia GS, Dinca EB, Ozawa T, Kimura ET, McDermott MW, James CD, VandenBerg SR, Lal A (2008). An orthotopic skull base model of malignant meningioma. **Brain Pathology, 18(2): 172-179**.

Baia GS, Slocum A, Hyer JD, Misra A, Sehati N, VandenBerg SR, Feuerstein BG, Deen DF, McDermott MW, Lal A (2005). A genetic strategy to overcome the senescence of primary meningioma cell cultures. **Journal of Neuroncology, 78(2):113-121**.

Baia GS, Stifani S, Kimura ET, McDermott MW, Pieper RO, Lal A (2008). Notch activation is associated with tetraploidy and enhanced chromosomal instability in meningiomas. **Neoplasia, 10(6):604-612**.

Berry LW, Westmund B, Schedl T (1997). Germ-line tumor formation caused by activation of *glp-1*, a *Caenorhabditis elegans* member of Notch family of receptors. **Development, 124:925-936**.

Boström J, Meyer-Puttlitz B, Wolter M, Blaschke B, Weber RG, Lichter P, Ichimura K, Collins VP, Reifenberger G (2001). Alterations of the tumor supressor genes *CDKN2A*(INK4a/p16;p14ARF), *CDKN2B*(INK4b/p15) and *CDKN2C*(INK3c/p18) in atypical and anaplastic meningiomas. **American Journal of Pathology, 159(2):661-669**.

Bray SJ (2006). Notch signaling: a simple pathway becomes complex. **Nature Reviews Molecular Cell Biology, 7(9):678-689**.

CBTRUS (2008). Statistical report: primary brain tumors in the United States, 2000-2004- Years of Data Collected. **Central Brain Tumor Registry of the United States**.

Cuevas IC, Slocum A, Jun P, Costello JF, Bollen AW, Riggins GJ, McDermott MW, Lal A (2005). Meningioma transcript profiles reveal deregulated Notch signaling pathway. **Cancer Research, 65(12):5070-5075**.

Cushing H (1922). The meningioma (dural endotheliomas): their source and favored seats of origin. **Brain, 45:282-316**.

DeMonte F, Marmor E, Al-Mefty O (2001). Meningiomas *In:* Kaye AH & LawsJr ER (eds) **Brain Tumors**, an encyclopedic approach, Churchill Livingstone, 2nd Edition, 721-750.

Dinca, E.B., Sarkaria, J.N., Schroeder, M.A., Carlson, B.L., Voicu, R., Gupta, N., Berger, M.S., James, C.D. (2007). Bioluminescence monitoring of intracranial glioblastoma xenograft: response to primary and salvage temozolomide therapy. **Journal of Neurosurgery, 107(3):610-616**.

Fisher AL,Ohsako S, Caudy M (1996). The WRPW motif of the hairy-related basic helix-loop-helix repressor proteins acts as a 4-amino-acid transcription repression and protein-protein interaction domain. **Molecular & Cell Biology, 16:2670-2677**.

Fiuza UM & Arias AM (2007). Cell and molecular biology of Notch. **Journal of Endocrinology, (194):459-474**.

Geigl JB, Obenauf AC, Schwarzbraun T, Speicher MR (2008). Defining chromosomal instability. **Trends in Gentetics, (2):64-69**.

Greene, HS & Arnold, H (1945). The homologous and heterologous transplantation of brain and brain tumors. **Journal of Neurosurgery, 2:315-329**.

Gutmann DH, Donahoe J, Perry A, Lemke N, Gorse K, Kittiniyom K, Rempel SA, Gutierrez JA, Newsham IF (2000). Loss of DAL-1, a protein 4.1-related tumor supressor, is an important early event in the pathogenesis of meningiomas. **Human Molecular Genetics, 9:1495-1500**.

Gutmann DH & Giovannini M (2002). Mouse models of Neurofibromatosis 1 and 2. **Neoplasia, 4(4):279-290**.

Gutmann, D.H., Baker, S.J., Giovannini, M., Garbow, J., Weiss, W. (2003). Mouse models of human cancer consortium symposium on nervous system tumors. **Cancer Research, 63(11):3001-3004**.

Henrique D, Hirsinger E, Adam J, LeRoux I, Pourquie O, Ish-Horowicz D, Lewis J (1997). Maintenance of neuroepithelial progenitor cells by Delta-Notch signalling in the embryonic chick retina. **Current Biology, 7(9):661-670**.

Ikeda K, Saeki Y, Gonzalez-Agosti C, Ramesh V, Chiocca EA (1999). Inhibition of NF2-negative and NF2-positive primary human meningioma cell proliferation by overexpression of merlin due to vector-mediated transfer. **Journal of Neurosurgery, 91:85-92**.

Jensen, RL, Leppla, D, Rokosz, N, Wurster, RD (1998). Matrigel augments xenograft transplantation of meningioma cells into athymic mice. **Neurosurgery, 42(1):130-135**.

Junqueira JC & Carneiro J (2005). Nerve tissue & the nervous system. *In:* **Basic Histology, 11th Edition**,The McGraw-Hill Companies, 161-190.

Kalamarides, MK, Stemmer-Rachamimov, AO, Takahashi, M, Han ZY, Chareyre, F, Niwa-Kawakita, M, Black, PM, Carroll, RS, Giovannini, M. (2008). Natural history of meningioma development in mice reveals: a synergy of Nf2 and p16(Ink4a) mutations. **Brain Pathology, 18(1):62-70**.

Kalamarides, MK, Niwa-Kawakita, M, Leblois,H, Abramowski, V, Perricadet, M, Janin, A, Thomas, G, Gutmann, DH, Giovannini, M. (2002). Nf2 gene inactivation in arachnoidal cells is rate-limiting for meningioma development in the mouse. **Genes and Development, 16(9):1060-1065**.

Keppes JJ. (1986). Presidential address: the histology of meningiomas. A reflection of origins and expected behavior? **Journal of Neuropathological and Experimental Neurology, 45:95-107**.

Ketter R, Henn W, Nieddermanyer I, Steilen-Gimbel H, Konig J, Sanz KD, Steudel WI (2001). Predictive value of progression-associated chromosomal aberrations for the prognosis of meningiomas: a retrospective study of 198 cases. **Journal of Neurosurgery, 95:601-607**.

Kopan R, (2002). Notch: a membrane-bound transcription factor. **Journal of Cell Science, 115(6):1095-1097**.

Lamszus K, Kluwe L, Matschke J, Meissner H, Lass R, Westphal M. (1999) Allelic losses at 1p, 9q, 10q, 14q and 22q in the progression of aggressive meningiomas and undifferentiated meningeal sarcomas. **Cancer Genetics and Cytogenetics, 110(2):103-110**.

Lamszus K, Meningioma pathology, genetics and biology (2004). **Journal of Neuropathology and Experimental Neurology, 63:275-286**.

Leong HG & Karsan A, (2006) . Recent insights into the role of Notch signaling in tumorigensis. **Blood, 107(6):2223-2233**.

Lundkvist J & Lendahl U, (2001). Notch and the birth of glial cells. **Trends in Neuroscience, 24:492-494**.

Luo D, Renault VM, Rando TA (2005). The regulation of Notch signaling in muscle stem cell activation and postnatal myogenesis. **Seminars in Cell & Developmental Biology, 16:612-622**.

Lusis E & Gutman DH (2004). Meningiomas: an update. **Current Opinion in Neurology, 17:687-692**.

Maxwell M, Shih SD, Galanopoulos T, Hedley-Whyte ET, Cosgrove GR (1998). Familial meningioma: analysis of expression of neurofibromatosis 2 protein Merlin. **Journal of Neurosurgery, 88(3):562-569**.

Medhkour, A, VanRoey, M, Sobel, RA Finger, HJ, Lee, J, Martuza, RL (1989). Implantation of human meningiomas into the subrenal capsule of the nude mouse. A model for studies of tumor growth. **Journal of Neurosurgery, 71:545-550**.

McCutcheon IE, Friend KE, Gerdes TM, Zhang BM, Wildrick DM, Fuller GN (2000). Intracranial injection of human meningioma cells in athymice mice: an orthotopic model for meningioma growth. **Journal of Neurosurgery, 92(2):306-314**.

Miele L (2006). Notch signaling. **Clinical Cancer Research, 12(4):1074-1079**.

Muller P, Henn W, Niedemayer I, Ketter R, Feiden W, Steudel WI, Zang KD, Steilen-Gimbel H (1999). Deletion of chromosome 1p and loss of expression of alkaline phosphatase indicate progression of meningiomas. **Clinical Cancer Research, 5:3569-3577**.

Olson, JJ, Beck, DW, Schlechte, JA, Loh, PM (1987). Effect of the antiprogesterone RU-38486 on meningioma implanted into nude mice. **Journal of Neurosurgery, 66:584-587**.

Perry A, Jenkins RB, Dahl RJ, Moertel CA, Scheithauer BW (1996). Cytogenetic analysis of aggressive meningiomas: possible diagnostic and prognostic implications. **Cancer, 77:2567-2573**.

Perry A, Scheithauer BW, Stafford SL, Lohse CM, Wollan PC. (1999). "Malignancy" in meningiomas: a clinicopathologic study of 116 patients, with grading implications. **Cancer, 85:2046-56**.

Perry A, Banerjee R, Lohse CM, Kleinschmidt-DeMasters, Scheithauer BW (2002). A role for chromosome 9p21 deletions in the malignant progression of meningiomas and the prognosis of anaplastic meningiomas. **Brain Pathology, 12:183-190**.

Perry A, Gutmann DH, Reifenberger G (2004). Molecular pathogenesis of meningiomas. **Journal of Neurooncology, 70:183-202**.

Perry A, Louis DN, Scheithauer BW, Budka H, vonDeimling A, (2007). Meningiomas *In:* Louis DN, Ohgaki H, Wiestler OD, Cavenee WK (eds) **WHO Classification of the Central Nervous System**, WHO Press, 4th Edition, 164-177.

Peterson DL, Sheridan PJ, Brown WJr (1994) Animal models for brain tumors: historical perspectives and future directions. **Journal of Neurosurgery, 80(5):865-876**.

Puttmann S, Senner V, Braune S, Hillmann B, Exeler R, Rickert CH, Paulus W (2006). Establishment of a benign meningioma cell line by hTERT-mediated immortalization. **Laboratory Investigation, 85(9):1163-1171**.

Qi R, An H, Yu Y, Zhang M, Liu S, Xu H, Guo Z, Cheng T, Cao X (2003). Notch1 signaling inhibits growth of human hepatocellular carcinoma through induction of cell cycle arrest and apoptosis. **Cancer Research, 63:8223-8329**.

Ragel BT, Elam IL, Gillespie DL, Flynn JR, Kelly DA, Mabey D, Feng H, Couldwell WT, Jensen RL. (2008) A novel model of intracranial meningioma in mice using luciferase-expressing meningioma cells. **Journal of Neurosurgery, 108(2):304-310**.

Ragel, BT & Jensen RL (2005). Molecular genetics of meningiomas. **Neurosurgery Focus, 19(5):1-8**.

Ragel, BT, Couldwell, WT, Gillespie, DL, Wendland, MM, Whang, K, Jensen, RL. (2008) A comparison of the cell lines used in meningioma research. **Surgical Neurology 70(3):295-307**.

Rana MW, Pinkerton H, Thornton H, Nagy D. (1977). Heterotransplantation of human glioblastoma multiforme and meningioma to nude mice. **Proceedings of the Society for Experimental Biology and Medicine, 155(1):85-88**.

Riemenschneider M, Perry A, Reifenberger G (2006). Histological classification and molecular genetics of meningiomas. **The Lancet Neurology, 5(12):1045-1054**.

Rouleau GA, Wertelecki W, Haines JL, Hobbs WJ, Trofatter JA, Seizinger BR, Martuza RL, Superneau DW, Conneally PM, Gusella JF (1987). Genetic linkeage of bilateral acoustic neurofibromatosis to a DNA marker on chromosome 22. **Nature, 329:246-248**.

Rouleau GA, Merel P, Lutchman M, Sanson M, Zucman J, Marineau C, Hoang-Xuan K, Demczuk S, Desmaze C, Plougastel B, *et al.* (1993). Alteration in a new gene encoding a putative membrave-organizing protein causes neurofibromatosis type 2. **Nature, 363(6429): 495-496**.

Roy M, Pear WS, Aster JC (2007). The multifaceted role of Notch in cancer. **Current Opinion in Genetics & Development, (17):52-59**.

Sadetzki S, Flint-Richter P, Ben-Tal T, Nass D (2002). Radiation-induced meningioma: a descriptive study of 253 cases. **Journal of Neurosurgery, 97(5):1078-1082**.

Sato A, Klaunberg B, Tolwani R (2004). *In vivo* bioluminescence imaging. **Comparative Medicine, 54(6):631-634**.

Sayagues JM, Tabernero MD, Maillo A, Diaz P, Rasillo A, Bortoluci A, Gomez-Moreta J, Santos-Briz A, Morales F, Orfao A. (2002). Incidence of numerical chromosome

aberrations in meningioma tumors as revealed by fluorescence in situ hybridization using 10 chromosome-specific probes. **Cytometry, 50(3):153-159**.

Shaw RJ, Paez JG, Curto M, Yaktine A, Pruitt WM, Saotome I, O'Bryan JP, Gupta V, Ratner N, Der CJ, Jacks T, McClatchey AI (2001) The NF2 tumor supressor, Merlin functions in Rac-dependent signaliing. **Developmental Cell, (1):63-72**.

Shcherbata HR, Althauser C, Findley SD, Ruohola-Baker H. (2004). The mitotic to endocycle switch in *Drosophila* follicle cells is executed by Notch-dependent regulation of G1/S, G2/M and M/G1 cell-cycle transitions. **Development, 131:3169-3181**.

Shou J, Ross S, Koeppen H, deSauvage FJ, Gao WQ (2001). Dynamics of notch expression during murine prostate development and tumorigenesis. **Cancer Research, 61:7291-7297**.

Simon T, Park TW, Koster G, Mahlberg R, Hackernbroch M, Bostrom J, Loning T, Schramm J. (2001). Alterations of INK4a(p16—p14ARF)/INK4b(p15) expression and telomerase activation in meningioma progression. **Journal of Neurooncology, 55:149-158**.

Singh N, Phillips RA, Iscove NN, Egan SE (2000). Expression of notch receptors, notch ligands, and fringe genes in hematopoiesis. **Experimental Hematology, 28:527-534**.

Storchova Z & Pellman D (2004). From polyploidy to aneuploidy, genome instability and cancer. **Nature Reviews in Molecular Cell Biology, 5(1)45-54**.

Sun L, Tap P, Yap C, Hwang W, Koh LP, Lim CK, Aw SE (2004). *In vitro* biological characteristics of human cord blood-derived megakaryocytes. **Annals Academy of Medicine of Singapore, 33:570-757**.

Szentirmai O, Baker CH, Lin N, Szucs S, Takahashi M, Kiryu S, Kung AL, Mulligan RC, Carter BS (2006). Noninvasive bioluminescence imaging of luciferase expressing intracranial U87 xenografts: correlation with magnetic resonance imaging determined tumor volume and longitudinal use in assessing tumor growth and antiangiogenice treatment effect. **Neurosurgery, 58:365-372**.

Trofatter JA, MacCollin MM, Rutter JL, Murrell JR, Duyao MP, Parry DM, Eldridge R, Kley N, Menon AG, Pulaski K, *et al.* (1993). A novel moesin-, ezrin-, radixin-like gene is a candidate for the neurofibromatosis 2 tumor suppressor. **Cell, 72(5):791-800**.

VanFurth WR, Laughlin S, Taylor MD, Salhia B, Mainprize T, Henkelman M, Cusimano MD, Ackerley C, Rutka JT (2003). Imaging of murine brain tumors using a 1.5 Tesla clinical MRI system. **The Canadian Journal of Neurological Sciences, 30(4):326-332**.

VanTiborg AG, Velthuizen SC, deVries A, Kros JM, Avezaat CJ, deKlein A, Beverloo HB, Zwarthoff EC (2005). Chromosomal instability in meningiomas. **Journal of Neuropathology and Experimental Neurology, 64(4):312-322**.

Vogel HB & Berry RG (1975). Chorioallantoic membrane herero-transplantation of human brain tumors. **International Journal of Cancer, 15:401-408**.

Weissleder R & Ntziachristos V (2003). Shedding light onto live molecular targets. **Nature Medicine, 9(1):123-128**.

Weng AP, Ferrando AA, Lee W, Morris JP, Silverman LB, Sanchez-Irizarry C, Blacklow SC, Look AT, Aster JC (2004). Activating mutations of Notch1 in human T-cell acute lymphoblastic leukemia. **Science, 306:269-271**.

Yan B, Raben N, Plotz PH (2002). Hes-1, a known transcriptional repressior, acts as a transcriptional activator for the human acid alpha-glucosidase gene in human fibroblast cells. **Biochemical and Biophysical Research Communications, 291: 582-587**.